JACS
JOURNAL OF THE AMERICAN CHEMICAL SOCIETY

Communication

pubs.acs.org/JACS

In Situ Reaction Monitoring Reveals a Diastereoselective Ligand Exchange Reaction between the Intrinsically Chiral $Au_{38}(SR)_{24}$ and Chiral Thiols

Stefan Knoppe,[†] Raymond Azoulay,[†] Amala Dass,[‡] and Thomas Bürgi*[,†]

[†]Department of Physical Chemistry, University of Geneva, 30 Quai Ernest-Ansermet, 1211 Geneva 4, Switzerland

[‡]Department of Chemistry and Biochemistry, University of Mississippi, 352 Coulter Hall, Oxford, Mississippi 38677, United States

Supporting Information

ABSTRACT: The ligand exchange reaction between racemic $Au_{38}(2\text{-PET})_{24}$ (2-PET = 2-phenylethylthiolate) clusters and enantiopure 1,1′-binaphthyl-2,2′-dithiol (BINAS) was monitored *in situ* using a chiral high-performance liquid chromatography approach. In the first exchange step, a clear preference of *R*-BINAS for the left-handed enantiomer of $Au_{38}(2\text{-PET})_{24}$ is observed (about 4 times faster than reaction with the right-handed enantiomer). The second exchange step is much slower than the first step. BINAS substitution deactivates the cluster for further exchange, which is attributed to (stereo)electronic effects. The results constitute the first example of a ligand exchange reaction in a thiolate-protected gold cluster with directed enrichment of a defined species in the product mixture. This may open new possibilities for the design of nanomaterials with tailored properties.

Ligand exchange reactions are commonly used for postsynthetic functionalization of gold clusters.[1−3] Choice of ligand and control over the reaction conditions allow tailoring of optical (e.g., fluorescence)[4,5] and electrochemical properties,[6] incorporation into liquid crystals,[1,2] and tuning of solubility.[7] Although quite detailed information on ligand exchange has been gained recently,[8] no attention has been paid until now to the influence of the handedness of the particles or clusters, despite the fact that intrinsic chirality was found to be a common feature of such clusters.[9−13] For example, the crystal structures of $Au_{102}(p\text{-MBA})_{44}$ (*p*-MBA = *para*-mercaptobenzoic acid) and $Au_{38}(2\text{-PET})_{24}$ (2-PET = 2-phenylethylthiolate) reveal a chiral arrangement of the protecting ligands on the cluster surface.[10,11] Since the ligands are achiral, the clusters are racemic in the crystals.

We studied the ligand exchange reaction between $Au_{38}(2\text{-PET})_{24}$ and $Au_{40}(2\text{-PET})_{24}$ clusters and the bidentate, axially chiral 1,1′-binaphthyl-2,2′-dithiol (BINAS) ligand[14,15] using circular dichroism and matrix-assisted laser desorption/ionization mass spectrometry (MALDI-MS).[14] It was found that two 2-PET ligands are replaced by one BINAS ligand. Furthermore, exchange reactions on pure Au_{38} and Au_{40} clusters revealed strong nonlinearities between arising optical activity and the average number of chiral ligands in the cluster samples,[15] which was explained by the intrinsic chirality of these clusters.

The chirality of $Au_{38}(SR)_{24}$ is based on the fact that the protecting staple motifs are arranged in a chiral fashion.[11,12] Two triblade fans, each composed of three dimeric staples, protect the "poles" of the cluster. The fans have the same handedness, thus leading to a chiral structure. The remaining three monomeric staple motifs are arranged around the equator. The two enantiomers of the clusters have been labeled as L (left-handed) and D (right-handed),[11,15−17] but we prefer to use the descriptors *A* (anticlockwise, left-handed) and *C* (clockwise, right-handed), which were proposed for the description of chirality in coordination polyhedrons.[18] L and D are usually used to describe central chirality, but the chiral feature we discuss is due to the arrangement of the protecting ligands.

Here we report for the first time a diastereoselective thiolate-for-thiolate ligand exchange reaction observed when the enantiomers of $Au_{38}(2\text{-PET})_{24}$ reacted with enantiopure *R*-BINAS (Figure 1). *rac*-$Au_{38}(2\text{-PET})_{24}$ clusters were prepared and isolated as described previously.[14,19−21] The UV−vis and MALDI-MS spectra are in agreement with Au_{38} clusters (not shown).[21−23] The chiral high-performance liquid chromatography (HPLC) shows only two peaks with the same area at 8.85 and 17.10 min, indicating monodispersity of the clusters and a true racemate.[24] We performed ligand exchange using *R*-BINAS and monitored the reaction *in situ* by HPLC. For convenience, the following notation is used: (*A*/*C*-38, 24 − 2*x*, *R*-*x*), where *A*/*C*-38 are *A*- or *C*-$Au_{38}(SR)_{24}$, 24 − 2*x* is the number of 2-PET ligands, and *R*-*x* denotes the number of *R*-BINAS ligands.

At short reaction times (up to ca. 15 h), two new peaks evolve (Figure 2, left), which are assigned to the exchange products with $x = 1$, (*A*-38, 22, *R*-1) and (*C*-38, 22, *R*-1), in agreement with the finding that no $x = 2$ species are found in mass spectra at rather short reaction times.[14,15] Evolution of peak areas with time allows us to assign the absolute configuration of the exchanged products since we know the handedness of the starting material. The *A*-enantiomer decreases faster than the *C*-enantiomer. Accordingly, the peak area of the third species, eluting at 24 min, increases faster than the area of the fourth band, at 33 min. Thus, we assume that

Received: October 19, 2012
Published: December 6, 2012

   dx.doi.org/10.1021/ja310330m | *J. Am. Chem. Soc.* 2012, 134, 20302−20305

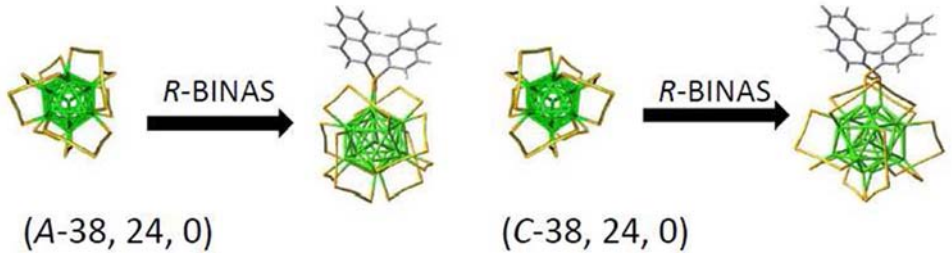

Figure 1. Schematic representation of the ligand exchange reaction between racemic $Au_{38}(SCH_2CH_2Ph)_{24}$ and *R*-BINAS. The $-SCH_2CH_2Ph$ groups were removed for clarity. Colors: green, Au_{Core}; yellow, Au_{Adatom}; orange, sulfur; gray, carbon; white, hydrogen. It is assumed that BINAS reacts selectively with the monomeric staples at the equator of the cluster (regioselectivity). The structures in the left equation represent the left-handed *A*-enantiomer (*A* = anticlockwise), and the structures in the equation on the right represent the right-handed *C*-enantiomer (*C* = clockwise). The products on the right-hand side are diastereomeric: *A*-$Au_{38}(SCH_2CH_2Ph)_{22}(R\text{-BINAS})_1$ and *C*-$Au_{38}(SCH_2CH_2Ph)_{22}(R\text{-BINAS})_1$. The structures of the Au_{38} core and staples were extracted from the crystal structure data in ref 11. Note that the structures containing BINAS were *not* optimized and are shown here for illustration purposes.

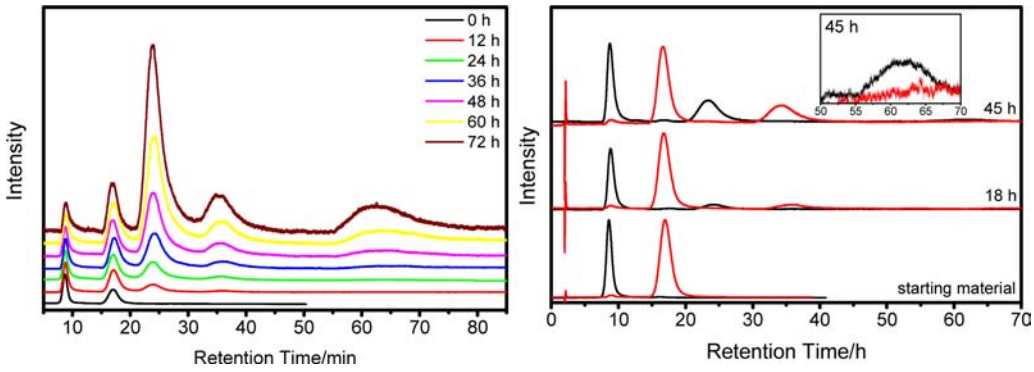

Figure 2. (Left) Exemplary HPLC (0−72 h) of the ligand exchange reaction between *rac*-$Au_{38}(2\text{-PET})_{24}$ and *R*-BINAS. The detector wavelength was set to 630 nm to avoid contribution from BINAS to the overall absorbance. Chromatograms were normalized to the peak at 8.96 min, which is (*A*-38, 24, 0). In comparison, the signal of (*C*-38, 24, 0) at 17.08 min increases in intensity over time. This indicates that (*A*-38, 24, 0) is consumed faster. The peak at 24.02 min is assigned to (*A*-38, 22, *R*-1), and the peak at 35.53 min is expected to be (*C*-38, 22, *R*-1). It is obvious that (*A*-38, 22, *R*-1) is produced much faster than (*C*-38, 22, *R*-1). The signal at 63.22 min appears at longer reaction times and is tentatively assigned to (*A*-38, 20, *R*-2). (Right) Chromatograms prior to and at 18 and 45 h of reaction times for reaction between *R*-BINAS and the pure enantiomers. Black traces, *A*-$Au_{38}(2\text{-PET})_{24}$; red traces, *C*-$Au_{38}(2\text{-PET})_{24}$. The chromatograms are complementary and serve as further proof for the assignment of the reaction products.

the third species is (*A*-38, 22, *R*-1) and the fourth species is (*C*-38, 22, *R*-1). At increasing reaction times, a new band centered at 63 min was observed. This band is broad and low in intensity. We assume that this signal is the second exchange of the *A*-enantiomer, (*A*-38, 20, *R*-2). Since the exchange with the *C*-enantiomer is slow, the corresponding $x = 2$ species is not observed, even at extended reaction times. In order to validate the peak assignment made above, the reactions were repeated starting from the separated enantiomers.[24] Since we do not expect racemization or interconversion during the reaction, the chromatograms should be complementary, depending on the enantiomer of Au_{38} used in the reaction. This was indeed found (Figure 2, right) and thus confirms the assignment of the peaks, which are listed in Table 1.

The system studied can be described by the following two consecutive independent reactions:

$$(A\text{-}38,\ 24,\ R\text{-}0) + 2R\text{-BINAS} \rightarrow (A\text{-}38,\ 22,\ R\text{-}1) + R\text{-BINAS} \rightarrow (A\text{-}38,\ 20,\ R\text{-}2)$$

and

$$(C\text{-}38,\ 24,\ R\text{-}0) + 2R\text{-BINAS} \rightarrow (C\text{-}38,\ 22,\ R\text{-}1) + R\text{-BINAS} \rightarrow (C\text{-}38,\ 20,\ R\text{-}2)$$

Table 1. Retention Times and Assignment of the Bands Observed in HPLC of the Ligand Exchange between *rac*-$Au_{38}(2\text{-PET})_{24}$ and *R*-BINAS

peak no.	retention time (min)	assignment
1	8.96	(*A*-38, 24, 0)
2	17.08	(*C*-38, 24, 0)
3	24.02	(*A*-38, 22, *R*-1)
4	35.53	(*C*-38, 22, *R*-1)
5	63.22	(*A*-38, 20, *R*-2)

The kinetics can be analyzed quantitatively, assuming that, at the detection wavelengths of the HPLC (630 nm), the exchanged and unexchanged species have the same absorption coefficient. This seems justified, as the incorporation of BINAS has only minor influence on the UV−vis spectra at longer wavelengths.[15] The rate constants k_1 and k_2 for the first and second ligand exchanges ($x = 0 \rightarrow x = 1$ and $x = 1 \rightarrow x = 2$) for the two reaction pathways were determined. In the following, the rate constants are highlighted with the handedness of the two starting enantiomers ($k^A_{1/2}$ and $k^C_{1/2}$, respectively). At high excesses of the BINAS ligand with respect to the clusters, we can assume its concentration is constant, and the reaction is of pseudo-first-order with respect to the cluster.

dx.doi.org/10.1021/ja310330m | J. Am. Chem. Soc. 2012, 134, 20302−20305

The total concentrations in a peak set were normalized to unity, and the relative concentrations were determined and used for a fit, shown in Figure 3 (nonlinear curve-fitting, least-

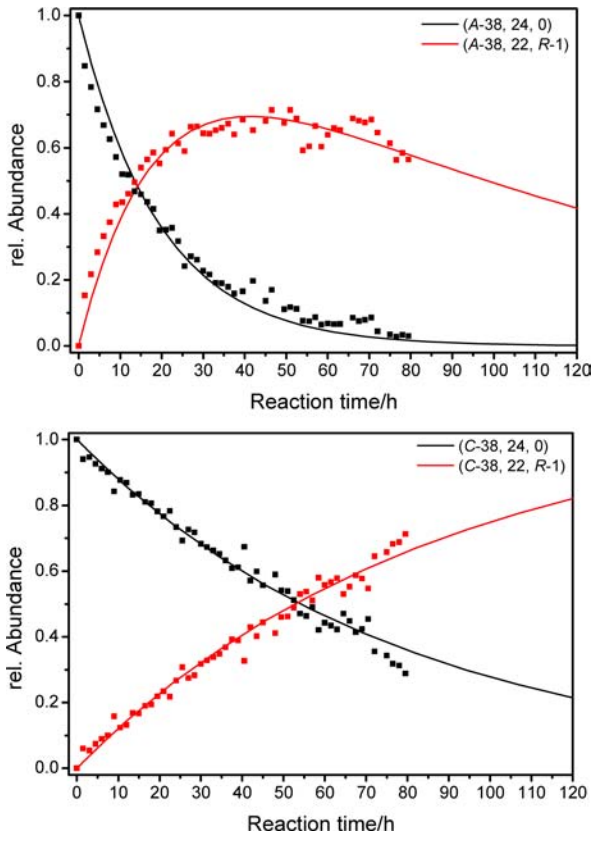

Figure 3. Kinetic fits for the *A* (top) and *C* (bottom) pathways. The dots are the values as determined from HPLC experiments, the traces are the corresponding fits (compare text). Black dots refer to the initial cluster, whereas red dots represent the first exchange product. The latter has a maximum at ca. 40 h for the *A*-pathway, after which the rate of the second exchange step, leading to (*A*-38, 20, *R*-2), begins to dominate the reaction. In direct comparison, it becomes obvious that the reaction is faster for the left-handed (*A*) isomer. The concentrations of (38, 24, 0) and (38, 22, *R*-1) are equal at 14.5 and 54 h, respectively (intersection of the curves).

squares using MATLAB R2011B from MathWorks, Natick, MA; the program code is included in the SI). The extracted rate constants are listed in Table 2. Since the reaction is drastically

Table 2. First-Order Rate Constants (in h^{-1}) for the Ligand Exchange between *rac*-$Au_{38}(2\text{-PET})_{24}$ and *R*-BINAS for the First and Second Exchange Steps

	A pathway	*C* pathway
k_1	0.0514 ± 0.0019 (3.8%)	0.0128 ± 0.0003 (2.6%)
k_2	0.0088 ± 0.0006 (6.9%)	not interpretable

slower for the *C*-isomer of the cluster, the errors of the corresponding rate constants are bigger, especially k_2^C. The value for k_2^C therefore could not be determined. The other rate constants (k_1^A, k_2^A, and k_1^C) can be determined with errors below 7%. Comparison of k_1^A (0.0514 h^{-1}) and k_1^C (0.0128 h^{-1}) shows that the reaction is about 4 times faster for the *A*-isomer, indicating that the reaction is diastereoselective (one of the diastereomers of the product is preferably formed). This is in agreement with the observed relative peak areas of (*A*-38, 22, *R*-1) and (*C*-38, 22, *R*-1) in the HPLC, which is about 4:1. This corresponds to a diastereomeric excess of 60%. To the best of our knowledge, this is the first time that diastereoselective ligand exchange in thiolate-protected gold clusters has been demonstrated. For the faster-reacting isomer (left-handed cluster), the rate constants for the second exchange could also be determined. The first exchange is ca. 5.8 times faster than the second exchange step (0.0514 vs 0.0088 h^{-1}), which is a surprisingly large difference. One part of this difference arises due to the fact that, after the first exchange, one site is already occupied. The number of equivalent exchange sites for BINAS is three if exchange takes place at the monomeric staples and six if it takes place at the dimeric staples. This leads to statistical factors of 2/3 and 5/6, respectively, for the second exchange with respect to the first one. Taking this statistical factor into account, the second exchange constant should be 0.0514 × 2/3 = 0.034 h^{-1} for exchange at the monomeric staples, which is still a factor of 3.9 higher than the measured rate. This factor of almost 4 is therefore attributed to steric and/or electronic reasons, meaning that the presence of one BINAS ligand slows down the intrinsic reaction rate constant considerably.

We would like to point out that the measured preference of *R*-BINAS toward the left-handed enantiomer of $Au_{38}(SR)_{24}$ is based on kinetic analysis of the reaction. The rate constants do not allow conclusions on the relative stability of the diastereomeric products formed. However, the observed rates could be a good test for the recently proposed generalized theoretical model of the ligand exchange.[8]

In conclusion, the ligand exchange between racemic $Au_{38}(2\text{-PET})_{24}$ and *R*-BINAS was shown to be diastereoselective, leading to preferential formation of (*A*-38, 22, *R*-1) compared to (*C*-38, 22, *R*-1). The exchange is about 4 times faster for the preferred enantiomer, leading to a diastereomeric excess of about 60%. The rate of the second exchange step is drastically lower (ca. 5.8 times). We ascribe this largely to electronic and/or steric effects. Ligand exchange reactions generally lead to a distribution of exchange products, but this work shows that exchange products such as *A*-$Au_{38}(SCH_2CH_2Ph)_{22}$(*R*-BINAS)$_1$ can be enriched in a mixture, which opens new possibilities for the design and preparation of atomically precise nanoscale objects. Future work will be devoted to the characterization of such species.

■ ASSOCIATED CONTENT

Supporting Information

Synthesis of R-BINAS, synthesis and size-selection of *rac*-$Au_{38}(2\text{-PET})_{24}$, HPLC method used for *in situ* monitoring, and the program code of the Matlab routine. This material is available free of charge via the Internet at http://pubs.acs.org.

■ AUTHOR INFORMATION

Corresponding Author

thomas.buergi@unige.ch

Notes

The authors declare no competing financial interest.

■ ACKNOWLEDGMENTS

We thank Dr. Igor Dolamic for help with the HPLC work. We acknowledge financial support from the Swiss National

Foundation, the University of Geneva (S.K., R.A., T.B.), and the University of Mississippi (A.D.).

REFERENCES

(1) Cseh, L.; Mehl, G. H. *J. Mater. Chem.* **2007**, *17*, 311.
(2) Frein, S.; Boudon, J.; Vonlanthen, M.; Scharf, T.; Barberá, J.; Süss-Fink, G.; Bürgi, T.; Deschenaux, R. *Helv. Chim. Acta* **2008**, *91*, 2321.
(3) Hostetler, M. J.; Green, S. J.; Stokes, J. J.; Murray, R. W. *J. Am. Chem. Soc.* **1996**, *118*, 4212.
(4) Shibu, E. S.; Muhammed, M. A. H.; Tsukuda, T.; Pradeep, T. *J. Phys. Chem. C* **2008**, *112*, 12168.
(5) Wang, G.; Huang, T.; Murray, R. W.; Menard, L.; Nuzzo, R. G. *J. Am. Chem. Soc.* **2005**, *127*, 812.
(6) Parker, J. F.; Kacprzak, K. A.; Lopez-Acevedo, O.; Häkkinen, H.; Murray, R. W. *J. Phys. Chem. C* **2010**, *114*, 8276.
(7) Pengo, P.; Polizzi, S.; Battagliarin, M.; Pasquato, L.; Scrimin, P. *J. Mater. Chem.* **2003**, *13*, 2471.
(8) Heinecke, C. L.; Ni, T. W.; Malola, S.; Makinen, V.; Wong, O. A.; Hakkinen, H.; Ackerson, C. J. *J. Am. Chem. Soc.* **2012**, *134*, 13316.
(9) Hakkinen, H. *Nat. Chem.* **2012**, *4*, 443.
(10) Jadzinsky, P. D.; Calero, G.; Ackerson, C. J.; Bushnell, D. A.; Kornberg, R. D. *Science* **2007**, *318*, 430.
(11) Qian, H.; Eckenhoff, W. T.; Zhu, Y.; Pintauer, T.; Jin, R. *J. Am. Chem. Soc.* **2010**, *132*, 8280.
(12) Lopez-Acevedo, O.; Tsunoyama, H.; Tsukuda, T.; Hakkinen, H.; Aikens, C. M. *J. Am. Chem. Soc.* **2010**, *132*, 8210.
(13) Tlahuice, A.; Garzon, I. L. *Phys. Chem. Chem. Phys.* **2012**, *14*, 3737.
(14) Knoppe, S.; Dharmaratne, A. C.; Schreiner, E.; Dass, A.; Burgi, T. *J. Am. Chem. Soc.* **2010**, *132*, 16783.
(15) Knoppe, S.; Dass, A.; Burgi, T. *Nanoscale* **2012**, *4*, 4211.
(16) Qian, H.; Zhu, M.; Wu, Z.; Jin, R. *Acc. Chem. Res.* **2012**, *45*, 1470.
(17) Knoppe, S.; Dolamic, I.; Burgi, T. *J. Am. Chem. Soc.* **2012**, *134*, 13114.
(18) Brown, M. F.; Cook, B. R.; Sloan, T. E. *Inorg. Chem.* **1975**, *14*, 1273.
(19) Knoppe, S.; Boudon, J.; Dolamic, I.; Dass, A.; Burgi, T. *Anal. Chem.* **2011**, *83*, 5056.
(20) Qian, H.; Zhu, M.; Andersen, U. N.; Jin, R. *J. Phys. Chem. A* **2009**, *113*, 4281.
(21) Qian, H.; Zhu, Y.; Jin, R. *ACS Nano* **2009**, *3*, 3795.
(22) Chaki, N. K.; Negishi, Y.; Tsunoyama, H.; Shichibu, Y.; Tsukuda, T. *J. Am. Chem. Soc.* **2008**, *130*, 8608.
(23) Toikkanen, O.; Ruiz, V.; Rönnholm, G.; Kalkkinen, N.; Liljeroth, P.; Quinn, B. M. *J. Am. Chem. Soc.* **2008**, *130*, 11049.
(24) Dolamic, I.; Knoppe, S.; Dass, A.; Bürgi, T. *Nat. Commun.* **2012**, *3*, 798.